

# Multifunctional Hydrophilic Poly(vinylidene fluoride) Graft Copolymer with Supertoughness and Supergluing Properties

Sanjoy Samanta, Dhruva P. Chatterjee, Swarup Manna, Amit Mandal, Ashesh Garai, and Arun K. Nandi\*

Polymer Science Unit, Indian Association for the Cultivation of Science, Jadavpur, Kolkata 700032, India

Received February 11, 2009; Revised Manuscript Received February 27, 2009

**ABSTRACT:** Here we report the grafting of *N,N*-dimethylaminoethyl methacrylate (DMAEMA) directly from poly(vinylidene fluoride) (PVDF) backbone in solution phase by atom transfer radical polymerization (ATRP). The graft length is same for different times of polymerization but graft density increases with increasing polymerization time. Four graft copolymers are prepared and depending on the time of conversion they are designated as PD-6, PD-12, PD-18, and PD-24, the number indicates time (h) of polymerization. A maximum of 36% (w/w) conversion with respect to monomer is achieved in the PD-24 sample. Gel permeation chromatography (GPC), nuclear magnetic resonance (NMR), and polymerization kinetics study conclude the ATRP nature of the polymerization. The graft copolymer shows induced solubility in water and the effective particle diameter in aqueous medium decreases from PD-6 to PD-24 samples. The enthalpy of fusion values are same in graft copolymers with more than 50% reduction and the melting points reduce by 5–6 °C than that of pure PVDF. WAXS patterns of graft copolymers indicate the formation of mixture of  $\alpha$  and  $\beta$  phases in dimethyl formamide cast films and also suggest the existence of self-organized short-range ordering from supramolecular interaction between the  $>C=O$  group and the nitrogen atom of the substituted amino group of the grafting component as is evident from the FTIR study. The absence of any lamellar peak than that of pure PVDF in the SAXS data suggests the formation of fringed micelle crystals in the graft copolymers. Storage modulus of graft copolymers decreases more than that of PVDF due to a decrease in crystallinity. The tensile stress–strain experiment of the PD samples indicates 700–750% elongation, which is 45 times higher than that of PVDF. The toughness increases by 1970% in the graft copolymers over that of pure PVDF, and the gluing property is significantly larger. The graft copolymers produce and stabilize gold nanoparticles in aqueous medium; produce amphiphilic membranes and on its modification to trimethyl ammonium ion it shows  $2.2 \times 10^{-6}$  S/cm dc-conductivity. Because of its water solubility, the polymer promises great use in biotechnology, nanotechnology, energy research, and separation processes.

## Introduction

Achieving enhanced physical and mechanical properties of commercial polymeric materials by blending with other polymers,<sup>1–3</sup> copolymerizing with other monomers,<sup>4–6</sup> grafting of the main chain with suitable polymeric/oligomeric moiety<sup>7–9</sup> and making composites with nanofillers, e.g.; clay, carbon nanotubes, metal nanoparticles, etc.,<sup>–14</sup> has been the main thrust in polymer materials research for the past few decades. Such materials are needed to fulfill the increasing specific demands of polymer technologists, biomedical engineers, nanotechnologists, electronics, and optoelectronics materialists. Poly(vinylidene fluoride) (PVDF) is a technologically important polymer because of its significant piezo and pyroelectric properties,<sup>15</sup> good biocompatibility,<sup>16</sup> excellent membrane forming capability,<sup>8,17</sup> etc. Grafting of this hydrophobic polymer with hydrophilic monomer exhibits enhanced surface properties, i.e., wettability, antifouling property, biocompatibility, and antistaticity.<sup>8,16,17</sup> We applied a new strategy to improve the physical and mechanical properties of this important polymer using supramolecular interactions for versatile applications with *N,N*-dimethylaminoethyl methacrylate (DMAEMA) having important interacting sites capable of forming self-assembly. Besides DMAEMA is an amphiphilic monomer and it produces a low  $T_g$  amorphous homopolymer, so the graft copolymer having micro crystallites of PVDF may produce interesting physical, biological and mechanical properties. Also new properties may develop from the self-organization through the interacting sites of the grafted chains promising to be a multifunctional polymeric material.

There are some reports of grafting PVDF mainly with hydrophilic monomers e.g. oxyethylene methacrylate (OEM), *tert*-butyl methacrylate as precursor of methacrylic acid,<sup>8,18,19</sup> and DMAEMA<sup>20</sup> using different techniques. With increasing graft conversion, the hydrophilicity and antifouling property of grafted PVDF increases.<sup>8,19,20</sup> The amphiphilic graft copolymers of PVDF finds specific use in membrane science, particularly in pH sensitive separation technique.<sup>8</sup> However, not much attention is yet given to the mechanical, adhesion and solubility properties of these polymers particularly for PVDF-*g*-DMAEMA copolymer that promises its multidimensional use in materials science. Among the different methods of grafting by free radical polymerization, atom transfer radical polymerization (ATRP) is gaining importance for the robust nature of the process that overcomes the homopolymerization of comonomer, backbone degradation, gel formation etc. Chen et al. used ATRP technique for grafting DMAEMA on *solid PVDF surface* in aqueous medium which would certainly result in a very low degree of grafting.<sup>20</sup> This type of *surface grafting* only modify surface properties but not the bulk properties of the system. Here, we report a new method of grafting DMAEMA on *PVDF backbone using solution phase PVDF*, to obtain a significant grafting density that develops self-assembling interactions producing a supertough, superglue and water soluble PVDF with multidimensional applications.

## Experimental Section

**Samples.** PVDF (Aldrich,  $M_n = 7.0 \times 10^4$ , polydispersity index 2.57, head to head (H–H) defect = 4.33 mol %) was purified by recrystallization from its 0.2% (w/w) solution of acetophenone. The monomer DMAEMA (Acros Organics, New Jersey) was purified

\* Corresponding author. E-mail: psuakn@mahendra.iacs.res.in.

by passing through basic alumina column. *N*-Methyl-2-pyrrolidone (NMP) and tetrahydrofuran (THF) were purchased from Loba Chemicals, Mumbai, India and were distilled and stored in argon atmosphere. 4,4'-dimethyl-2,2'-dipyridyl (DMDP), ethyl-2-bromo isobutyrate (EBiB) and cuprous chloride (CuCl) were purchased from Aldrich Chemical Co. USA. CuCl was purified by washing with 10% HCl in water followed by methanol and diethyl ether in a Schlenk tube under a nitrogen atmosphere.

**Polymerization. Preparation of Graft Copolymer.** In a nitrogen purged tube ( $8 \times 2.5$  cm) containing 20% (w/v) NMP solution of PVDF, 4,4'-dimethyl-2,2'-dipyridyl (DMDP) and cuprous chloride (CuCl) were added. The mole ratio of PVDF, DMDP and CuCl was 0.07:3.2:1. DMAEMA (volume ratio of NMP and DMAEMA 1.25:1) was next introduced into the tube, and nitrogen purging was continued for 15 min after which the tube was closed with a rubber septum. The mixture was stirred magnetically for 30 min to prepare a homogeneous solution. The tube was then placed in an oil bath (90 °C) followed by stirring. For kinetic studies, separate experiments were performed for different times. After the desired time period, the contents of the tube were diluted with 1 mL of NMP and poured into petroleum ether (60–80 °C). The separated polymer was isolated, redissolved in NMP, and precipitated into excess petroleum ether. The polymer was dried in vacuum at 40 °C and then washed repeatedly with double distilled water followed by drying in vacuum at room temperature. The resulting polymer was weighed and the percent monomer conversion was calculated. There were 18, 25, 31, 36, 37, and 36% conversion for 6, 12, 18, 24, 36, and 48 h of polymerization. The theoretical molecular weights were obtained by multiplying the target molecular weight (amount of monomer in g/amount of PVDF in mol)<sup>21</sup> with percent conversion calculated from gravimetric technique. The theoretical values are 1.17, 1.35, 1.51,  $1.64 \times 10^5$ , and  $1.7 \times 10^5$  for PD-6, PD-12, PD-18, PD-24, and PD-36 samples (numbers denote the time (h) of polymerization).

**Preparation of Homopolymer.** To a nitrogen purged tube ( $8 \times 2.5$  cm) containing 3.6 mL of acetone, 0.4 mL of double distilled water, 0.0198 g of CuCl, 0.062 g of 2,2'-bipyridyl and 0.029 mL of ethyl-2-bromo isobutyrate were taken. Nitrogen purging was continued for 15 min after which the tube was closed with a rubber septum. DMAEMA (4 mL) was next introduced into the tube with a nitrogen purged gastight syringe. The mixture was stirred magnetically at room temperature. After 24 h, the contents of the tube were diluted with excess THF, passed through silica gel column and stored in a R.B. After solvent evaporation, the polymer was dissolved in minimum amount of THF and precipitated by petroleum ether. The separated polymer was isolated, redissolved in THF and reprecipitated by petroleum ether followed by drying in vacuum at 40 °C.

**Characterization. Gel Permeation Chromatography.** The gel permeation chromatography (GPC) experiments were made using a Waters instrument with a  $\mu$ -Styragel column in DMF solvent using a refractive index detector. The sample was eluted with 1% (w/v) LiNO<sub>3</sub> in DMF at a flow rate of 0.5 mL/min.

**Dynamic Light Scattering Studies.** The effective particle sizes of aqueous solutions of PD samples were measured using a Dynamic Light Scattering instrument (Brookhaven Instruments Corporation, Model BI-APD).

**Spectral Characterization.** The <sup>1</sup>H NMR spectra of the reaction products were made in DMSO-*d*<sub>6</sub> on a 300 MHz Bruker instrument. The <sup>1</sup>H NMR spectra was used to calculate the graft length and graft density of the graft copolymer. The <sup>19</sup>F NMR spectra was performed with a 300 MHz Bruker instrument at the Central Drug Research Institute (CDRI), Lucknow, India. A 6–8% polymer solution was prepared in *N,N*-dimethylformamide-*d*<sub>7</sub> (DMF-*d*<sub>7</sub>) and the spectra was recorded without proton decoupling.<sup>22</sup> The <sup>19</sup>F NMR spectra was analyzed with a seven-carbon sequence<sup>23,24</sup> and the head to head (H–H) defects were calculated by the method of Wilson and Santee.<sup>25</sup> The FT-IR spectra of the samples were

obtained on a Shimadzu FT-IR instrument using polymer thin films cast from DMF.

**X-ray Scattering.** The WAXS data were taken from the DMF cast films by a Seifert X-ray diffractometer model (C 300) in reflection mode with a parallel beam optics attachment. Nickel-filtered copper K $\alpha$  radiation ( $\lambda = 0.154$  nm) operating at a 35 kV voltage and a 30 mA current was used. The samples on Al holder were scanned from  $2\theta = 2^\circ$  to  $37^\circ$  at the step scan mode (step size  $0.03^\circ$ , preset time 2 s) and the diffraction pattern was recorded using a scintillation counter detector. The SAXS data were taken from a Bruker Nanostar 2D SAXS Instrument with rotating anode generator using Cu K $\alpha$  radiation and a 2D Gadds detector at the National Chemical Laboratory, PUNE.

**Microscopy.** SEM study of the DMF cast films of PD samples were made using a scanning electron microscope (Jeol GSM-5800). The samples were platinum coated prior observation.

**Thermal Study.** The melting point and enthalpy of fusion data of the graft copolymers were measured by a Perkin-Elmer differential scanning calorimeter (DSC) (Diamond DSC-7) working under nitrogen atmosphere. It was calibrated with indium before each set of experiment. Weighed samples ( $\sim 3$  mg) were crimped by a universal crimper. They were heated from  $-30$  to  $+200$  °C at  $10$  °C/min. The melting temperature and enthalpy of fusion values were measured with the help of a personal computer attached to the instrument. The cooling experiments were made by cooling the samples from the melt at the cooling rate of  $5^\circ/\text{min}$ .

The thermal stability of the PD samples was measured using a TGA/DTA instrument (model SDT Q600, TA instrument) under nitrogen atmosphere at a heating rate of  $10$  °C/min.

**Mechanical Properties.** The storage modulus ( $G'$ ), loss modulus ( $G''$ ) and  $\tan \delta$  of the PD samples were measured using a dynamic mechanical analyzer (DMA) (TA instruments model Q-800). Films of  $25 \text{ mm} \times 5 \text{ mm} \times 0.15 \text{ mm}$  dimensions were cast from the polymer solution on a die made of polypropylene. These films were then installed in the tension clamp of the calibrated instrument. The sample was heated from  $-100$  to  $+150$  °C at a heating rate of  $10$  °C/min. The storage modulus, loss modulus, and  $\tan \delta$  were measured at a constant frequency of 1 Hz with static force of 0.02 N.

Tensile tests were carried out from DMF cast films of uniform thickness using a Zwick/Roell Universal Testing Machine (Z005) at a strain rate of  $1 \text{ mm min}^{-1}$  at room temperature (30 °C). Each experiment was repeated three times to observe reproducibility.

**Dc Conductivity Measurement.** The dc conductivity of the modified samples at 30 °C was measured by the standard - spring loaded pressure contact four-probe method. A circular film of 1.3 cm diameter was used and the probes were connected with the help of Ag paste. A constant current ( $I$ ) was passed from a direct current source electrometer (Keithley model 617) through two diagonal leads of the four probes and the voltage ( $V$ ) across the other two leads was measured using a multimeter (Keithley, model 2000). The conductivity ( $\sigma$ ) was calculated from the relation

$$\sigma = (\ln 2 / \pi d)(I/V) \quad (1)$$

where  $d$ , the thickness of the film was taken as the average of four measurements at different places using a screw gauge. Conductivity of two films each with two trials was measured and average of four such measurements was taken as the conductivity of the samples.

## Result and Discussion

**A. Characterization.** The synthesis of graft copolymer was carried out by ATRP in *N*-methylpyrrolidone (NMP) using cuprous chloride (CuCl) and 4,4'-dimethyl-2,2'-dipyridyl (DMDP) as catalyst and ligand, respectively. The characterization of the graft copolymers produced at different times, designated as PD-6, PD-12, PD-18, and PD-24 are made using NMR, GPC etc. The <sup>1</sup>H NMR spectra of PD-24, PVDF, and PDMAEMA are presented in Figure 1 and those of PD-6, PD-12, and PD-18

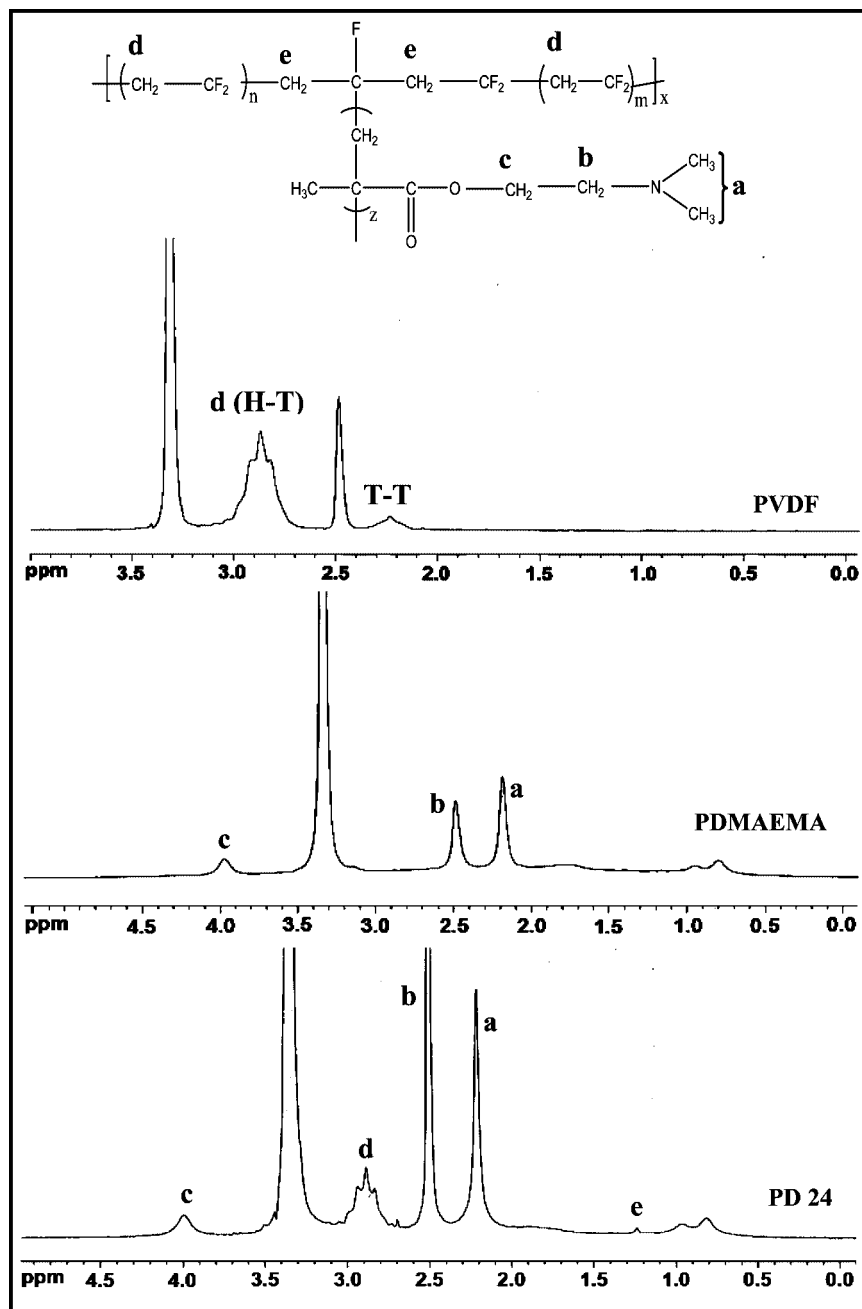


Figure 1.  $^1\text{H}$  NMR spectra of PD-24, PDMAEMA and PVDF in dimethyl- $d_6$  sulfoxide.

are presented in the Supporting Information Figure 1. Pure PVDF exhibits two main peaks at 2.23 and 2.85 ppm arising from  $>\text{CH}_2$  protons of tail-tail (T-T,  $-\text{CH}_2-\text{CH}_2-$ ) and head to tail (H-T,  $-\text{CF}_2-\text{CH}_2-$ ) linkages respectively.<sup>26a</sup> The peaks at 3.33 and 2.49 ppm are due to the moisture present in the solvent.<sup>26a,b</sup> The NMR spectra of PDMAEMA homopolymer indicates peaks at 2.19, 2.49, and 3.99 ppm corresponding to a, b and c protons<sup>27</sup> (Figure 1). The peak at 3.99 ppm (c) has been considered for the calculation of number average molecular weight of the grafted copolymer ( $M_{n,\text{graft}}$ ) using the equation

$$\bar{M}_{n,\text{graft}} = \bar{M}_{n,\text{PVDF}} \left( 1 + x \frac{M_0^{\text{comonomer}}}{M_0^{\text{PVDF}}} \right) \quad (2)$$

where  $x$  is the molar ratio of the comonomer units measured from NMR [ratio of area "c" with that of ( $\text{d} + 0.076\text{d} + \text{e}$ ),  $0.076\text{d}$  has been added for tail-tail protons] and  $M_0$ 's are the

molar masses of the respective unit. The observed  $M_{n,\text{graft}}$  values are 0.97, 1.14, 1.29, 1.42, and  $1.44 \times 10^5$  for PD-6, PD-12, PD-18, PD-24, and PD-36 respectively. The kinetic plot of  $\ln(m_0/m)$  ( $m_0$  is the initial monomer weight and  $m$  is the monomer weight at time  $t$ ) vs time (Figure 2a) indicates that first order kinetics is followed, at least up to 36% conversion (24 h of polymerization). In Figure 2b the molecular weight of the grafted chains are plotted with conversion and there is a linear increase up to 36% conversion. This indicates that ATRP mechanism is fully operating to produce PVDF-*g*-DMAEMA (PD) polymer at least up to 24 h of polymerization. This indicates living nature of grafted chain and hence the graft copolymers may be further used as macroinitiator for producing grafted block copolymers. The ratio  $M_{n,\text{graft}}/M_{n,\text{PVDF}}$  are presented in Table 1, and it increases with increase in polymerization time. The GPC traces of PVDF, PD-6, and PD-24 (Figure 2c) show clean sweep indicating absence of any termination reaction during grafting.

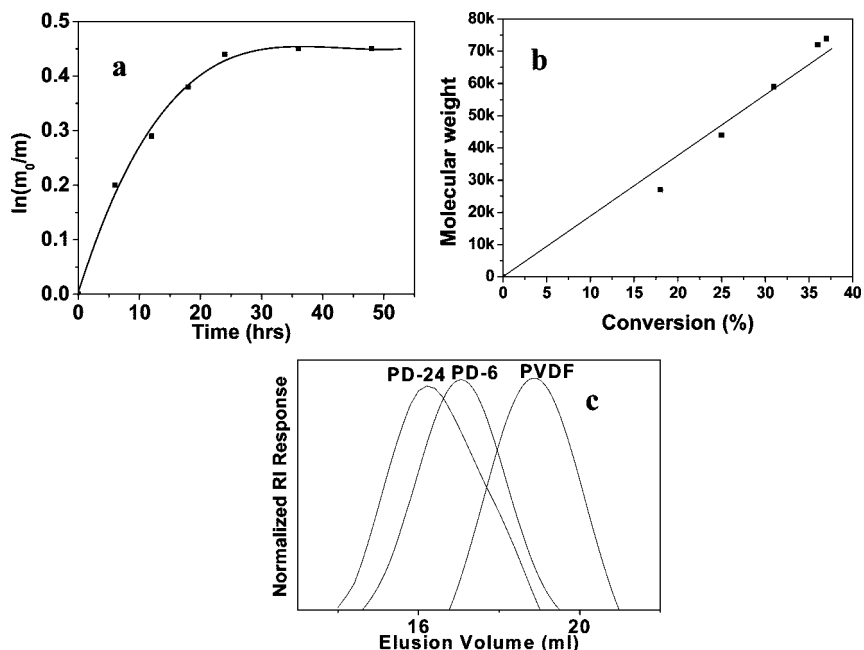


**Figure 2.** (a) Plot of monomer conversion ( $\ln m_0/m$ ) against time (h). (b) Plot of molecular weight of grafted chain vs monomer conversion. (c) GPC traces of PVDF, PD-6, and PD-24 samples.

**Table 1. Characteristics of PVDF and PD graft copolymers at 30°C**

sample	PVDF	PD-6	PD-12	PD-18	PD-24
$\bar{M}_{n, \text{graft}}/\bar{M}_{n, \text{PVDF}}$		1.4	1.6	1.8	2.0
$G'$ (MPa)	2310	970	856	924	588
strain % at break	16.5	715.6	751.9	705.7	698.9
stress at break (MPa)	6.0	20.7	15.2	20.9	11.2
toughness (N mm)	27.1	437.0	559.5	472.1	559.6
% increase of toughness		1518	1970	1648	1970

To calculate the average graft length and graft density the  $^1\text{H}$  NMR spectra was used. It is observed from the Figure 1 that the peak **e** newly arises in the grafted PVDF chain and it may be attributed for the  $>\text{CH}_2$  protons adjacent to the grafted carbon. Peak **c** is due to the  $-\text{O}-\text{CH}_2-$  protons of DMAEMA and it is not affected due to the presence of solvent. So normalizing the **c** and **e** peak areas for each proton, and taking the ratio, the average graft length has been calculated and is presented in Table 2. From the table, it is apparent that the average graft length is  $\sim 30$  DMAEMA units for all the samples. The average interval of grafting has been calculated from the ratio of (area **d** + 0.076**d**) with the area **e** normalized to single proton and the values are also presented in Table 2. The 0.076**d** has been added to account for the small contribution of tail–tail protons. It is apparent from the table that the average interval of grafting gradually decreases until 24 h of polymerization has taken place, indicating increasing initiating sites with the progress of reaction. Possibly during the grafting, the PVDF coil becomes gradually expanded for increased polarity of the chain making new  $>\text{CF}_2$  sites available for ATRP initiation. After 24 h. of reaction no more new grafting sites are produced. This may be attributed to the increased steric hindrance of grafted DMAEMA chains and increasing termination leading to lowering of active catalyst concentration. The average grafting sites per PVDF chain (may be termed as grafting density calculated from the ratio of degree of polymerization of PVDF and average interval of grafting) consequently increases till 24 h of polymerization but after that period grafting sites level up. The molecular weight of grafted DMAEMA is calculated by multiplying monomer molecular weight with (average grafting density  $\times$  average graft length). This molecular weights matches very well with those calculated directly from the ratio of total

$\text{CH}_2$  group peak area of PVDF and that of the **c** peak of DMAEMA, providing a cross checking of the different  $^1\text{H}$  NMR peak assignments used for the calculation of chain characteristics of grafted PVDF chain.

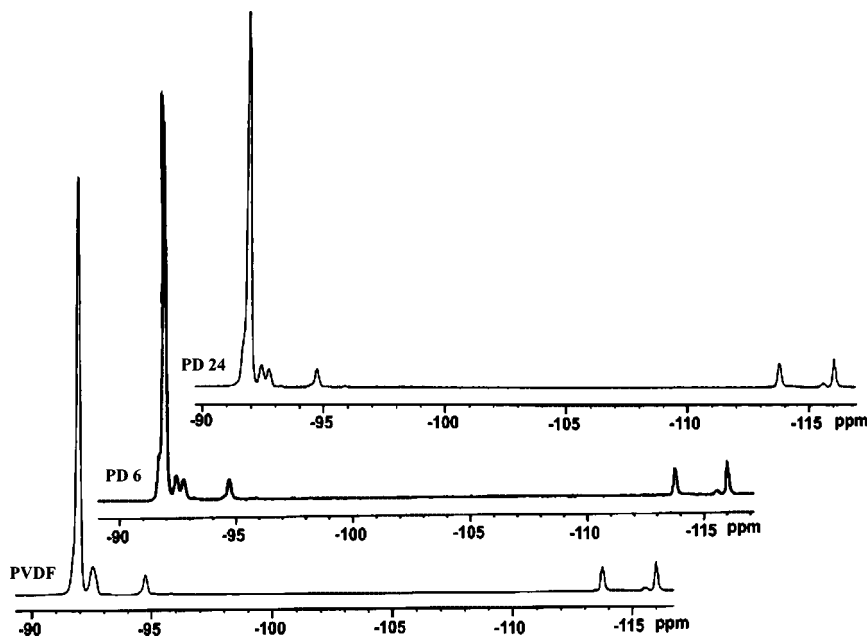
Now it would be interesting to find out the preferential sites of initiation, as PVDF has both head–tail ( $-\text{CF}_2-\text{CH}_2-$ , H–T) and head–head ( $-\text{CF}_2-\text{CF}_2-$ , H–H)  $>\text{CF}_2$  linkages. The correct determination of the H–H defect is possible from  $^{19}\text{F}$  NMR spectra (Figure 3) where the spectra of PVDF, PD-6, and PD-24 are presented. It is apparent from the figure that the 91.92, 92.51, 94.73, 113.74, 115.55, and 116 ppm peaks are for the  $>\text{CF}_2$  fluorine atoms being present at the center of the sequences; 0101010, 0101011, 1001010, 0101101, 1001100, and 1001101, respectively (0 =  $\text{CH}_2$  and 1 =  $\text{CF}_2$ ).<sup>24</sup> On grafting a new peak than those of PVDF arises at 92.74 ppm. This may be attributed for the central  $\text{CF}_2$  fluorine atoms experiencing different sequences than those presented above. Possibly it may arise due to the 100101 $^{1/2}$  sequence because on grafting at a  $\text{CF}_2$  unit it is converted into  $^{1/2}$  (i.e. a  $-\text{CF}_2-$ , g  $\Rightarrow$  graft chain). The new  $\text{CF}_2$  peak at 92.74 ppm which arises at the intermediate of 0101011 (91.79 ppm) and 1001010 (94.43 ppm)<sup>24</sup> may therefore appear for grafting. However, no new peak due to grafting is observed in the head–head (113–117 ppm) region because of the low concentration of the H–H defect. To find out the status of H–H defect during grafting, we calculated the H–H defect (mol %) from the method of Wilson and Santee<sup>22,25</sup> and the values of H–H defects are 4.33, 4.06, and 3.44 mol % for PVDF, PD-6, and PD-24, respectively. Thus H–H defects are gradually decreasing with increasing polymerization time and it may be argued that the preferential initiation center of grafting is at the H–H defect center. An analysis of  $^1\text{H}$  NMR data of table 2 and the present  $^{19}\text{F}$  NMR data may be useful to get an idea about the extent of grafting from the H–H and H–T  $>\text{CF}_2$  groups. From Table 2, it is apparent that in PD-6  $\sim 0.5$  mol % (100/191) of  $\text{VF}_2$  units are grafted while in PD-24  $\sim 1.4$  mol % (100/70)  $\text{VF}_2$  units are grafted. The decrease of H–H defect in PD-6 is 0.27 mol % and that in PD-24 is 0.89 mol % as obtained from  $^{19}\text{F}$  NMR spectral data. As 0.5 mol % grafting causes a decrease of the H–H defect by 0.27 mol %, consequently 54 mol % H–H units are grafted in PD-6. Similarly, 63% H–H units are grafted in PD-24 sample. So about 60% H–H units



**Table 2. Chain Characteristics of PVDF–DMAEMA Graft Copolymer Obtained from Analysis of  $^1\text{H}$  NMR Spectra in DMSO**

sample	normalized area of peak (au)			average			molecular weight of grafted DMAEMA	
	peak c	peak e	peak d	graft length	interval of grafting	grafting sites per PVDF chain (grafting density)	calculated <sup>a</sup>	obtained from the ratio of total area of PVDF–CH <sub>2</sub> group <sup>b</sup> and –O–CH <sub>2</sub> methylene group (e) of DMAEMA
PD-6	75	2.5	446	30.0	190.8	5.7	26 988	26 712
PD-12	62	2	223	31.0	119.3	9.2	44 630	43 894
PD-18	117	4	311	29.2	83.2	13.2	60 284	58 973
PD-24	256	8.5	556	30.1	70.0	15.6	73 815	71 865
PD-36	251	8.5	532	29.5	67.0	16.3	75 632	73 539

<sup>a</sup> Molecular weight is calculated as: monomer mol wt.  $\times$  graft length  $\times$  graft density. <sup>b</sup> The contribution of PVDF–CH<sub>2</sub> protons is calculated as follows: contribution of head-tail (H–T) protons + contribution of T–T protons (7.6% with respect to H–T) + contribution of e type protons.

**Figure 3.**  $^{19}\text{F}$  NMR spectra of PVDF, PD-6, and PD-24 samples in DMF- $d_7$ .

are attacked despite its much lower abundance (4.33 mol %) than that of H–T linkages (95.67%). As 60% H–H defects are grafted among the 4.33 mol % H–H defect present in the PVDF chain and 40% H–T linkages are grafted out of 95.67 mol % H–T linkages in the chain, so any new peak if appears at H–H region due to grafting would be of 15 (38.3/2.6) times lower intensity than that of the new peak appeared at 92.74 ppm. As a result such peaks are not observed at the H–H (113–117 ppm) region in the present  $^{19}\text{F}$  NMR spectra of the PD samples. The steric strain of H–H linkages are higher than that of H–T linkages [atomic radii of fluorine and hydrogen are 1.35 and 1.25 Å, respectively] causing the H–H sites to be vulnerable for catalyst ( $\text{Cu}^{\text{I}}\text{L}_n\text{X}$ ) attack in the ATRP method of polymerization. The difference in the amounts of T–T (3.8 mol %) and H–H defects (4.33 mol %) of PVDF, obtained from  $^1\text{H}$  and  $^{19}\text{F}$  NMR spectra, respectively, may be attributed to the Markovian statistics that PVDF chain usually follows.<sup>24,22b</sup>

**B. Hydrophilicity and Solubility.** The physical properties of the polymer are interesting because the hydrophilicity of PVDF increases appreciably due to grafting as it is evidenced from the gradual spreading of water drop on the graft copolymer film shown in Figure 4a. Also it exhibits *induced* solubility in water despite its hydrophobic backbone. Initially PD is dissolved in DMF (0.1% w/v) and on dilution by 40 times with water (usually considered as nonsolvent for PVDF) it remains in solution. After removing DMF by dialysis (10 kDa dialysis bag) for 5 days, the particle sizes are measured using dynamic light scattering (DLS) and the effective diameter values of PD-6, PD-12, PD-18, and PD-24 are 119, 107, 88, and 83 nm respectively, (Supporting Information Figure 2). The decrease in effective

diameter with increasing conversion may be due to the increased concentration of DMAEMA making the hydrophobic segments to be lesser aggregated causing smaller size particles. It is a first time report where a modified PVDF has been made completely soluble in water. In DMF, the self-organized structure of grafted copolymer (Figure 4b) is lost due to high solvating power of solvent and on its removal water solvates the hydrophilic side chains rendering PVDF backbone to be dissolved in water. In other words, the grafted DMAEMA render PVDF backbone to become solubilized in water.

**C. Thermal Property.** In the graft copolymers, the initial reduction of enthalpy of fusion (PD-6, 27 J/g) from that of pure PVDF (54 J/g) is certainly significant from the DSC thermograms (Figure 5a). The almost same enthalpy of fusion values, e.g., 20, 25, and 22 J/g for PD-12, PD-18, and PD-24, respectively, suggest that about six grafting sites per PVDF chain is sufficient to alter the crystallization behavior significantly. This is also supported from the invariant melting points of the graft copolymers though there is reduction of 5–6 °C from that of pure PVDF. The crystallization peak temperature decreases by 15–24 °C in the graft copolymers (Supporting Information Figure 3) than that of pure PVDF, and the decrease is greater with increasing graft conversion. As the graft length is same, the increased graft density put hindrance to the crystallization of intermediate vinylidene fluoride units causing a decrease in crystallization rate.

The TGA thermograms (Figure 5b) show a two stage degradation for both PDMAEMA and PD graft copolymers but pure PVDF shows a single stage degradation at 447.8 °C. The first stage degradation of PDMAEMA, PD-6, PD-12, PD-18,

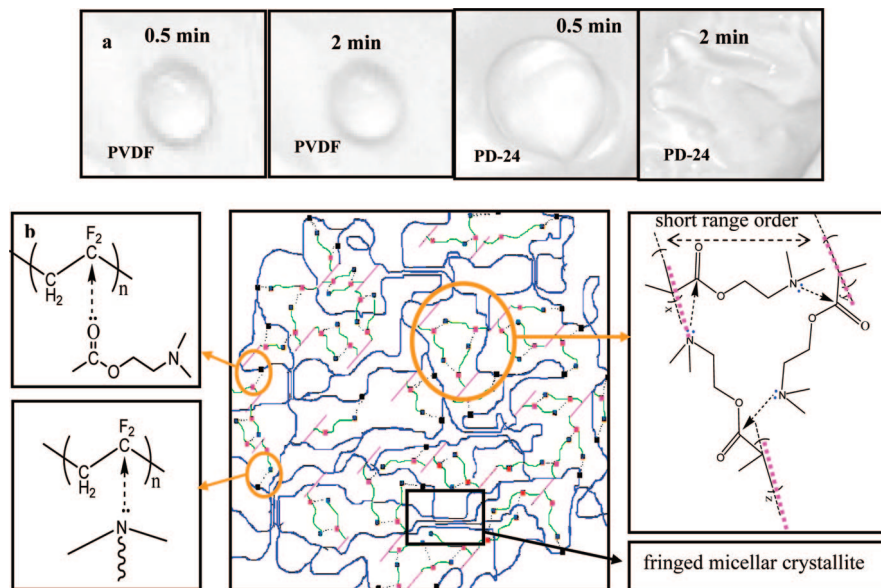


**Figure 4.** (a) Wettability test of PVDF and PD-24 films by dropping water on their DMF cast films for indicated times. (b) Schematic model of PVDF-g-DMAEMA graft chains with supramolecular interactions.

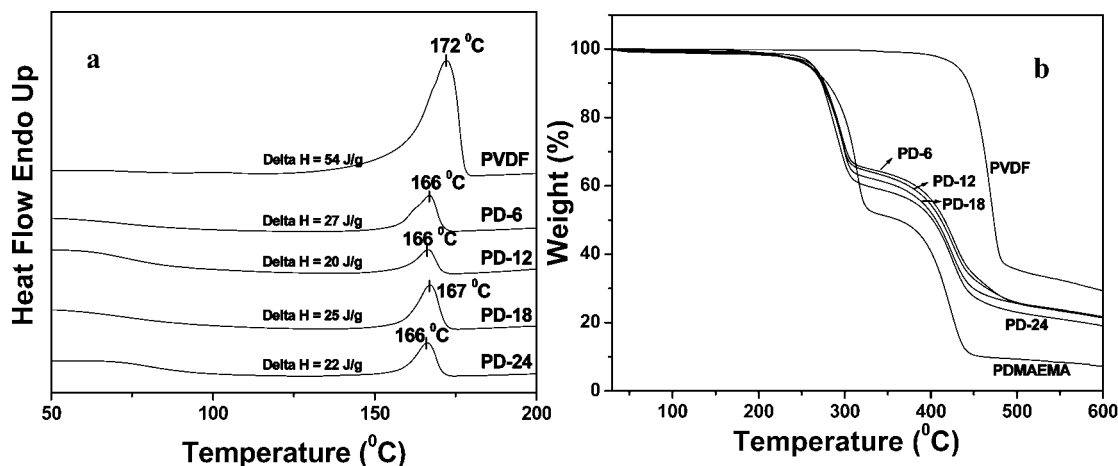


**Figure 5.** (a) DSC endotherms of PVDF and PD graft copolymers of DMF cast films at 10°/min heating rate. (b) TGA thermograms of PVDF and PD graft copolymers of DMF cast films at 10°/min heating rate under nitrogen atmosphere.

and PD-24 starts at 291, 269, 267, 266, and 274 °C respectively indicating degradation of graft copolymers occur earlier than that of PDMAEMA. The second stage of degradation is however constant at 396 °C for all cases. Possibly the side chain part containing dimethyl amino ethyl group degrades first through the ester linkage and the degradation of main chain methacrylate group occurs at the second stage. In the graft copolymers interaction of nonbonding electron pairs of nitrogen with the geminal fluorine atoms of  $>CF_2$  group of PVDF facilitates earlier degradation of dimethyl amino ethyl part of PDMAEMA. The degradation of PVDF fragments follows the same path as that of the attached methacrylate part of PDMAEMA showing an earlier degradation than that of pure PVDF.

**D. Structure.** The DMF cast films of PVDF produce mixture of  $\alpha$  and  $\beta$  polymorphs as evident from the WAXS peaks at  $2\theta = 18.5, 26.3^\circ$  for  $\alpha$  and  $20.2^\circ$  for  $\beta$  phase (Figure 6a) and it is also supported from the FTIR spectra (peaks at 797, 613, 530  $cm^{-1}$  (for  $\alpha$ ) and 839, 510 (for  $\beta$ )) (Supporting Information Figure 4).<sup>28</sup> It is important to note that the lower angle peak ( $2\theta = 7^\circ$ ) of WAXS pattern of PDMAEMA is broad which suggests the formation of a highly dispersed self-organized short-range ordering produced from supramolecular interactions of side chains. The ordering is stabilized through interchain

supramolecular interaction between tertiary amine N atom and C=O group (Figure 4b). In the WAXS pattern of the graft copolymers the same supramolecular ordering of side chains exist as evidenced from the lower angle WAXS peaks, though the presence of PVDF lowers the intensity. In Figure 6b SAXS patterns show that lamellar peak of PVDF is absent in PD-6 and PD-24 samples, suggesting the absence of chain folded lamellar crystals in the graft copolymers. Hence the crystallinity of the PD samples may arise due to the formation of fringed micelle crystals of the graft copolymers. The grafted chains hinder the chain folding process and the vacant VDF units may crystallize to produce fringed micellar crystallites (Figure 4b). The low crystallinity ( $\sim 20\%$ ) value of the PD graft copolymers supports the fringed micelle crystallization of PVDF.

A support of the above supramolecular interaction may be obtained from the  $>C=O$  peak positions ( $1724\text{--}1728\text{ cm}^{-1}$ ) which are  $7\text{--}11\text{ cm}^{-1}$  lower than that of ester carbonyl groups and also from the broader nature of the peaks (Figure 7). Also the above peak positions are  $4\text{--}8\text{ cm}^{-1}$  lower than that of the same polymer obtained from solid state ATRP<sup>20</sup> suggesting the presence of supramolecular interactions due to relatively higher grafting density in the present systems. The broad peak at  $2\theta \sim 17^\circ$  (Figure 6a) is due to the amorphous halo of the side

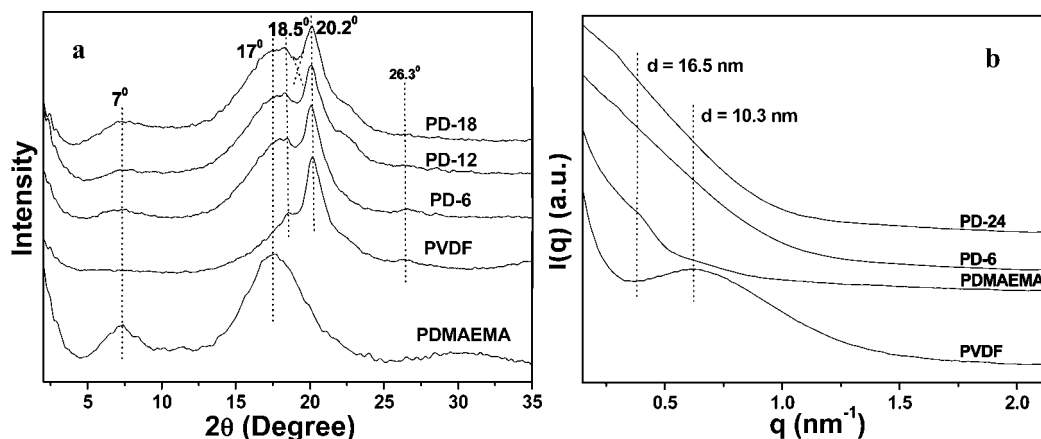


Figure 6. (a) WAXS patterns of PDMAEMA, PVDF, and PD samples. (b) SAXS patterns of PVDF, PDMAEMA, PD-6, and PD-24 samples.

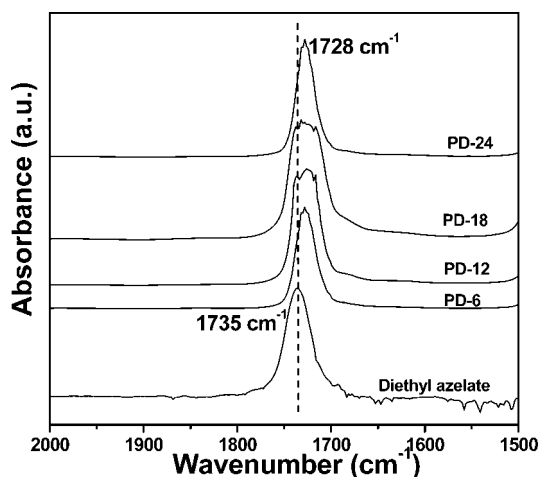


Figure 7. Comparison of FTIR spectral data of  $>\text{C}=\text{O}$  stretching vibration between an ester and the PD polymers showing supramolecular interactions.

chain and it also exists in the graft copolymers. The crystallite thickness, measured from Scherrer equation using the  $2\theta$  peak at  $20.2^\circ$  of deconvoluted WAXS pattern, indicate a reduction of crystallite size from 4.2 nm in PVDF to 3.2 nm in the graft copolymers. This 25% reduction in crystallite size occurs due to the rotational hindrance imposed by the grafted DMAEMA chain. The decrease of melting point of graft copolymers by  $5\text{--}6^\circ\text{C}$  from that of pure PVDF is due to the decrease of crystallite size.<sup>29</sup>

**E. Mechanical Properties.** In dynamic mechanical analysis of the PD polymers (Figure 8a,b), the glass transition temperature ( $T_g$ ) of PVDF is not observed, though pure PVDF exhibit  $T_g$  at  $-46^\circ\text{C}$  as evident from loss modulus peak.<sup>14</sup> The  $T_g$  of PDMAEMA is  $19^\circ\text{C}$ <sup>30</sup> and in the graft copolymers from the loss modulus plot the  $T_g$  (peak temperature) of PDMAEMA is also observed at  $18\text{--}22^\circ\text{C}$  indicating microphase separated system. The  $\tan \delta$  plots (Supporting Information Figure 5) also indicate the same  $T_g$  value of PDMAEMA in the graft copolymers ( $36\text{--}40^\circ\text{C}$ ). Thus it is a multiphase polymeric system containing mixture of  $\alpha$ - and  $\beta$ -PVDF crystalline phase, PVDF amorphous phase and the PDMAEMA self-organized phase. All the phases being in nanodimensions, interesting mechanical property is expected from this polymer. The storage modulus ( $G'$ ) of the graft copolymers decrease with both increase in temperature and increase in conversion (Figure 8a and Table 1). With increasing PDMAEMA in the chain the crystallinity reduces to a large extent, and there is also a lowering of crystallite size than that of pure PVDF. Decrease of crystallite

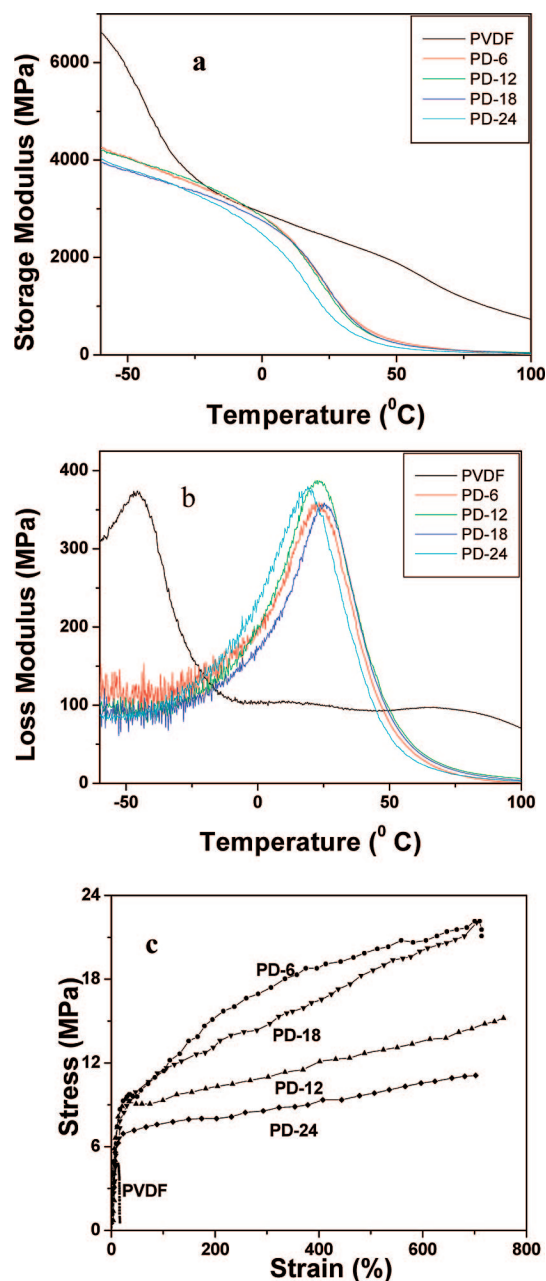
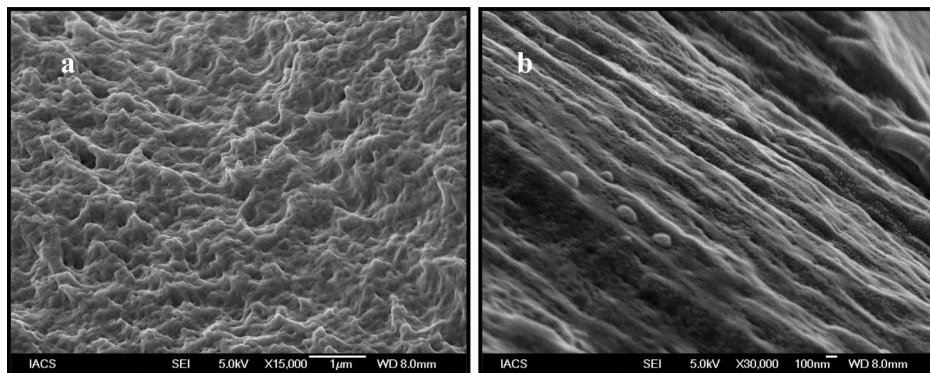


Figure 8. (a) Storage modulus and (b) loss modulus variation with temperature of PVDF and PD samples. (c) Stress–strain curve of PVDF and PD samples at  $30^\circ\text{C}$ .





**Figure 9.** (a) FE-SEM micrograph of DMF cast PD-24 film before drawing. (b) FE-SEM micrograph of DMF cast PD-24 film after drawing.

size would increase total surface area, so mechanical reinforcement should increase in graft copolymer. But the lowering of crystallinity by a substantial amount (>50%) overcomes the above reinforcement effect, causing an overall decrease in storage modulus with conversion. The decrease in  $G'$  with rise in temperature is for the increased chain mobility of both the main chain and the graft chain.<sup>31</sup> A large drop in  $G'$  from PVDF to graft copolymers at 30 °C is due to the easier energy dissipation for the initiation of side chain motions at this temperature which is 12 °C higher than the  $T_g$  of graft component.

Figure 8c compares the stress-strain curves of PVDF and the graft copolymers at a strain rate of 1 mm/min. The results are very exciting (Table 1) as in PVDF the elongation at break is 16.5%, while those of the graft copolymers is 700–750%. The increase of toughness in graft copolymers from that of PVDF is ~1970% and such a large increase is very unusual even when compared to the highest reported value (700%) for the modified nanoclay PVDF composite at room temperature.<sup>32</sup> The elongation at break is 45 times higher compared to that of pure PVDF. The FE-SEM morphology of the graft copolymer has fibrillar network structure (Figure 9a), mainly produced from self-organized structure present in the sample. On drawing, the network structure produces aligned fibrillar morphology which persists till its breaking (Figure 9b.) The breaking of supramolecular cross-links at DMAEMA brushes causes the unwinding of network structure into oriented fibers. So the supramolecular force of the pendent DMAEMA is mainly responsible for such dramatic increase of elongation and toughness in the sample. Also the soft DMAEMA nanodomains retard the growth of cracks by absorbing the stress leading to enhanced toughness. The mechanical properties of graft copolymers do not differ much despite their different grafting density and probably at the grafting density of six a reasonable number of supramolecular interactions take place affecting the mechanical properties to its optimum values.

**F. Adhesion Property.** Though the  $T_g$  of PVDF is very low (−46 °C), PVDF has no gluing property due to its high crystallinity, but grafting with DMAEMA imparts supergluing activity. In an experiment between two aluminum plates sandwiched with PD-24 sample (area = 1.47 cm<sup>2</sup>, thickness = 0.011 cm) can carry a load of 16 kg (Figure 10a). The gluing action is also tested between two glass slides and in both cases the supergluing activity is observed irrespective of nature of the surfaces. The PDMAEMA is tacky in nature due to its low  $T_g$  and self-organization ability of the polymer. So, the presence of DMAEMA is the cause of such adhesion in these graft copolymers, however the contribution of PVDF chain is certainly very large because PVDF nanocrystallites present in the system offer rigidity and strong attractive force due to their large surface area. Also during the heat treatment at 180 °C for

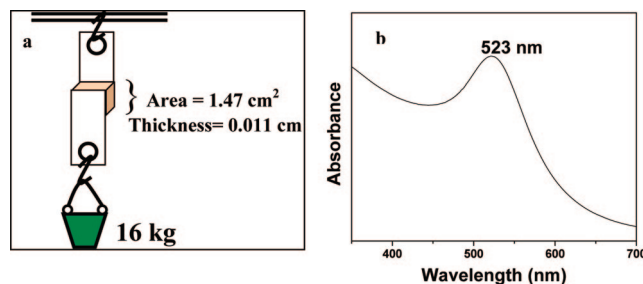


**Figure 10.** (a) Mechanical arrangement showing gluing ability measurement of PD-24 sample. (b) UV-vis spectrum of aqueous solution of gold nanoparticles produced from PD-24 and chloroauric acid.

gluing purpose some chemical cross-linking through nitrogen and geminal fluorine atoms is possible. The evidence of chemical cross-linking may be offered from the insolubility of the above glue in DMF, though PDMAEMA is soluble even after that heat treatment.

**G. Different Applications.** Due to its water solubility the PVDF-g-DMAEMA copolymer possess immense applications in materials research as it can be used to prepare nanoparticles in aqueous medium as evidenced from the UV-vis spectra (Figure 10b) of gold nanoparticles. This gold nanocomposite is produced by self-reducing property of *N,N*-dimethyl group on chloroauric acid solution and followed by stabilization with PVDF-g-DMAEMA.<sup>14</sup> The *N,N*-dimethyl group of the graft copolymer can be easily transformed into quaternary ammonium ions and the resulting polymer films have ionic conductivity of  $2.2 \times 10^{-6}$  S/cm that promises the possible use of the polymer in fuel cells as polymer electrolyte membrane.<sup>33</sup> The PD samples produce thermoreversible gels in different solvents and this polymer could certainly provide amphiphilic membranes to be useful for biological separation processes.<sup>34</sup> In a word, this super tough, superglue, water soluble PVDF-graft copolymer is highly attractive to materials scientists and technologists from different fields of engineering, nanotechnology, biotechnology and fuel cell applications.

## Conclusion

So, grafting of *N,N*-dimethylaminoethyl methacrylate (DMAEMA) directly from poly(vinylidene fluoride) (PVDF) backbone in solution phase by ATRP method yield graft copolymer of different graft density that depends on polymerization time up to 24 h. of polymerization. The graft lengths are however same for different polymerization time. The supramolecular interactions of the graft copolymer produce amphiphilic, supertough and supergluing polymeric material with multidimensional applications. The PD samples show 700–750% elongation, which is 45 times higher than that of PVDF and the toughness



increases by 1970% in the graft copolymers than that of pure PVDF. The gluing property is significantly large and a thin film (area = 1.47 cm<sup>2</sup>, thickness = 0.011 cm) of PD-24 can carry a load of 16 kg at 30 °C. The PD copolymers are useful to produce and stabilize gold nanoparticles in aqueous medium; modified to trimethyl ammonium ion show  $2.2 \times 10^{-6}$  S/cm dc-conductivity and produce amphiphilic membranes. It is a first time report where a modified PVDF has been made completely water soluble, and because of its water solubility, the polymer promises great use in biotechnology, nanotechnology, energy research, and separation processes.

**Acknowledgment.** We gratefully acknowledge Department of Science and Technology, New Delhi (Grant No. SR/SI/PS-32/2004) for financial support. We also thank Dr. C. Ramesh, NCL, Pune, India and Central Drug Research Institute, Lucknow, India, for helping in SAXS and <sup>19</sup>F NMR spectral measurements, respectively.

**Supporting Information Available:** Figures showing NMR, DLS, FTIR, DMA, and DSC thermograms of PVDF and PD samples. This material is available free of charge via the Internet at <http://pubs.acs.org>.

## References and Notes

- (1) *Multicomponent polymer materials*; Paul, D. H., Sperling, L. H., Eds.; American Chemical Society: Washington, DC, 1986.
- (2) Hu, B.; Karasz, F. E. *J. Appl. Phys.* **2003**, *93*, 1995.
- (3) *Multiphase Polymers: Blends and Ionomers*; Utracki, L. A., Weiss, R. A., Eds.; American Chemical Society: Washington, DC, 1989.
- (4) Hadjichristidis, N.; Pispas, S.; Floudas, G. A. *Block Copolymers. Synthetic Strategies, Physical Properties, and Applications*; Wiley-Interscience: New Jersey, 2003.
- (5) Thurn-Albrecht, T.; Schotter, J.; Kastle, G. A.; Emley, N.; Shibauchi, T.; Krusin-Elbaum, L.; Guarini, K.; Black, C. T.; Tuominen, M. T.; Russell, T. P. *Science* **2000**, *290*, 2126.
- (6) Nykanen, A.; Nuopponen, M.; Laukkanen, A.; Hirvonen, S.-P.; Rytela, M.; Turunen, O.; Tenhu, H.; Mezzenga, R.; Ikkala, O.; Ruokolainen, J. *Macromolecules* **2007**, *40*, 5827.
- (7) Neugebauer, D.; Zhang, Y.; Pakula, T.; Sheiko, S. S.; Matyjaszewski, K. *Macromolecules* **2003**, *36*, 6746.
- (8) Hester, J. F.; Banerjee, P.; Won, Y.-Y.; Akthakul, A.; Acar, M. H.; Mayes, A. M. *Macromolecules* **2002**, *35*, 7652.
- (9) Zhai, G.; Shi, Z. L.; Kang, E. T.; Neoh, K. G. *Macromol. Biosci.* **2005**, *5*, 974.
- (10) Giannelis, E. P.; Krishnamoorti, R.; Manias, E. *Adv. Polym. Sci.* **1999**, *138*, 107.
- (11) Ramanathan, T.; Abdala, A. A.; Stankovich, S.; Dikin, D. A.; Herrera-Alonso, M.; Piner, R. D.; Adamson, D. H.; Schniepp, H. C.; Chen, X.; Ruoff, R. S.; Nguyen, S. T.; Aksay, I. A.; Prud'homme, R. K.; Brinson, L. C. *Nat. Nanotechnol.* **2008**, *3*, 327.
- (12) Kuila, B. K.; Malik, S.; Batabyal, S. K.; Nandi, A. K. *Macromolecules* **2007**, *40*, 278.
- (13) Maiti, P.; Nam, P. H.; Okamoto, M. *Macromolecules* **2002**, *35*, 2042.
- (14) Manna, S.; Batabyal, S. K.; Nandi, A. K. *J. Phys. Chem. B* **2006**, *110*, 12318.
- (15) Lovinger, A. J. *Development in Crystalline Polymers— I*; Elsevier, Applied Science: London and New York, 1981.
- (16) Braga, F. J. C.; Rogero, S. O.; Couto, A. A. *Mater. Res.* **2007**, *10*, 247.
- (17) Chen, Y.; Ying, L.; Yu, W.; Kang, E. T.; Neoh, K. G. *Macromolecules* **2003**, *36*, 9451.
- (18) Liu, Y.; Lee, J. Y.; Kang, E. T.; Wang, P.; Tan, K. L. *React. Funct. Polym.* **2001**, *47*, 201.
- (19) Akthakul, A.; Salinaro, R. F.; Mayes, A. M. *Macromolecules* **2004**, *37*, 7663.
- (20) Chen, Y.; Liu, D.; Deng, Q.; He, X.; Wang, X. *J. Polym. Sci., Part A: Polym. Chem.* **2006**, *44*, 3434.
- (21) Matyjaszewski, K.; Jakubowski, W.; Min, K.; Tang, W.; Huang, J.; Braunecker, W. A.; Tsarevsky, N. V. *PNAS* **2006**, *103*, 15309.
- (22) (a) Nandi, A. K.; Mandelkern, L. *J. Polym. Sci., Part B: Polym. Phys.* **1991**, *29*, 1287. (b) Dikshit, A. K.; Nandi, A. K. *J. Polym. Sci., Part B: Polym. Phys.* **2000**, *38*, 297.
- (23) Ferguson, R. C.; Brame, E. G., Jr. *J. Phys. Chem.* **1979**, *83*, 11.
- (24) Cais, R. E.; Solane, N. J. A. *Polymer* **1983**, *24*, 179.
- (25) Wilson, C. W., III; Santee, E. R., Jr. *J. Polym. Sci.: Part C* **1965**, *8*, 97.
- (26) (a) Zhai, G.; Kang, E. T.; Neoh, K. G. *Macromolecules* **2004**, *37*, 7240. (b) Kim, Y. W.; Lee, D. K.; Lee, K. J.; Kim, J. H. *Eur. Polym. J.* **2008**, *44*, 932.
- (27) Baines, F. L.; Billingham, N. C.; Armes, S. P. *Macromolecules* **1996**, *29*, 3416.
- (28) Tashiro, K.; Kobayashi, M. *Phase Transitions* **1989**, *18*, 213.
- (29) Mandelkern, L. Crystallization and Melting In *Comprehensive Polymer Science*; Pergamon Press: Oxford, U.K., 1989; Vol. 2 p-363.
- (30) Jin, L.; Deng, Y.; Hu, J.; Wang, C. *J. Polym. Sci.: Part A: Polym. Chem.* **2004**, *42*, 6081.
- (31) Ferry, J. D. *Viscoelastic Properties of Polymers*; John Wiley and Sons: New York, 1961.
- (32) Shah, D.; Maiti, P.; Jiang, D. D.; Batt, C. A.; Giannelis, E. P. *Adv. Mater.* **2005**, *17*, 525.
- (33) Steele, B. C. H.; Heinzl, A. *Nature* **2001**, *414*, 345.
- (34) Taubert, A.; Napoli, A.; Meier, W. *Curr. Opin. Chem. Biol.* **2004**, *8*, 598.

MA9003117